Supplementary data

Measurement report: Characterizing O_3-NO_x-VOC sensitivity and O_3 formation in a heavily polluted central China megacity using multi-methods during 2019–2021 warm seasons

Shijie Yu [a], Hongyu Liu [a], Hui Wang [a]*， Fangcheng Su [b,c], Minghao Yuan [d], Ruiqin Zhang [b,c]**

a. Department of Environmental Engineering, Henan University of Science and Technology, Luoyang 471023, China

b. Institute of Environmental Sciences, Zhengzhou University, Zhengzhou 450001, China

c. School of Ecology and Environment, Zhengzhou University, Zhengzhou 450001, China

d. Environmental Protection Monitoring Center Station of Zhengzhou, Zhengzhou 450007, China

*Correspondence to: H. Wang, Department of Environmental Engineering, Henan University of Science and Technology, Luoyang, Henan, PR China, 471023

**Correspondence to: R. Zhang, Research Institute of Environmental Science, School of Ecology and Environment, Zhengzhou University, Zhengzhou, Henan, PR China, 450001

E-mail address: wanghui79@haust.edu.cn (H. Wang), rqzhang@zzu.edu.cn (R. Zhang)

Figure list

Table list:

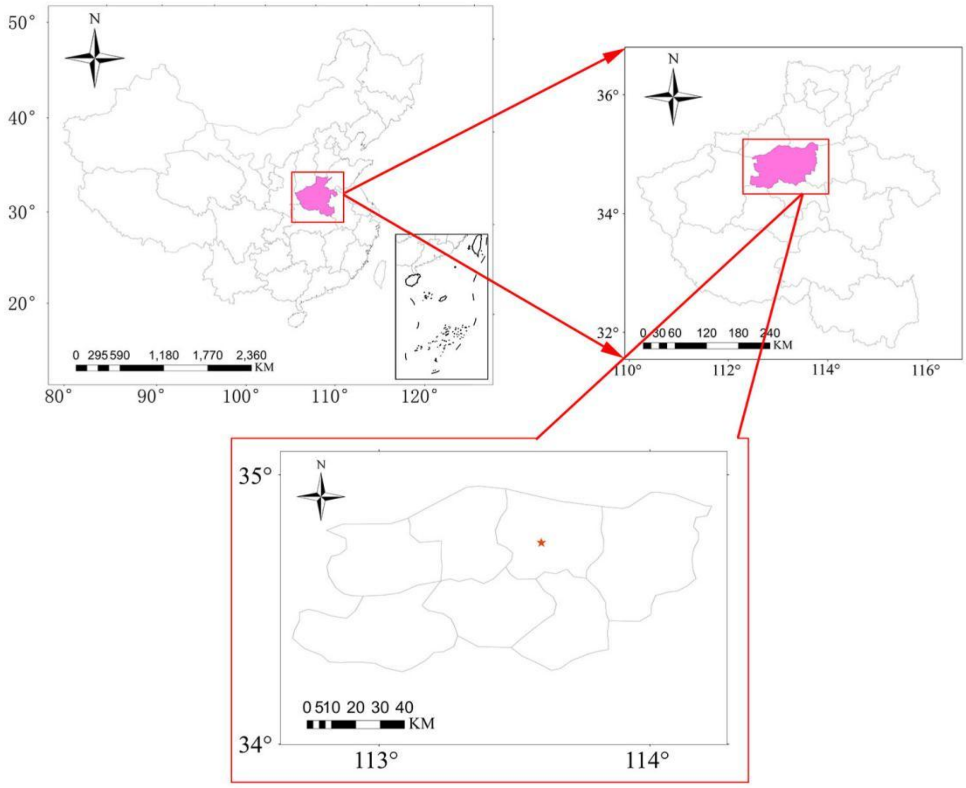

Fig. S1 Locations of the sampling stations in Zhengzhou.

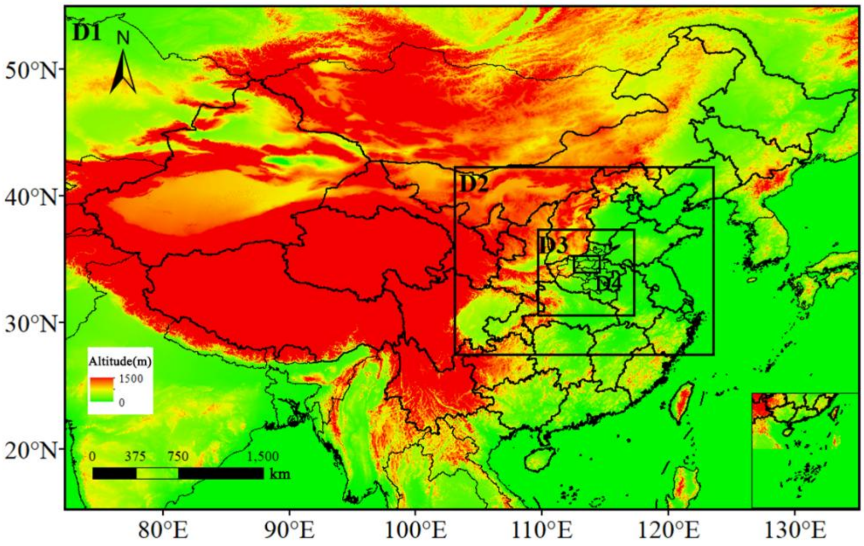

Fig. S2 Four-level nested domains used in the WRF/CMAQ simulations. D1, D2, D3 and D4 have horizontal resolutions of 36, 12, 4 and 1 km, respectively.

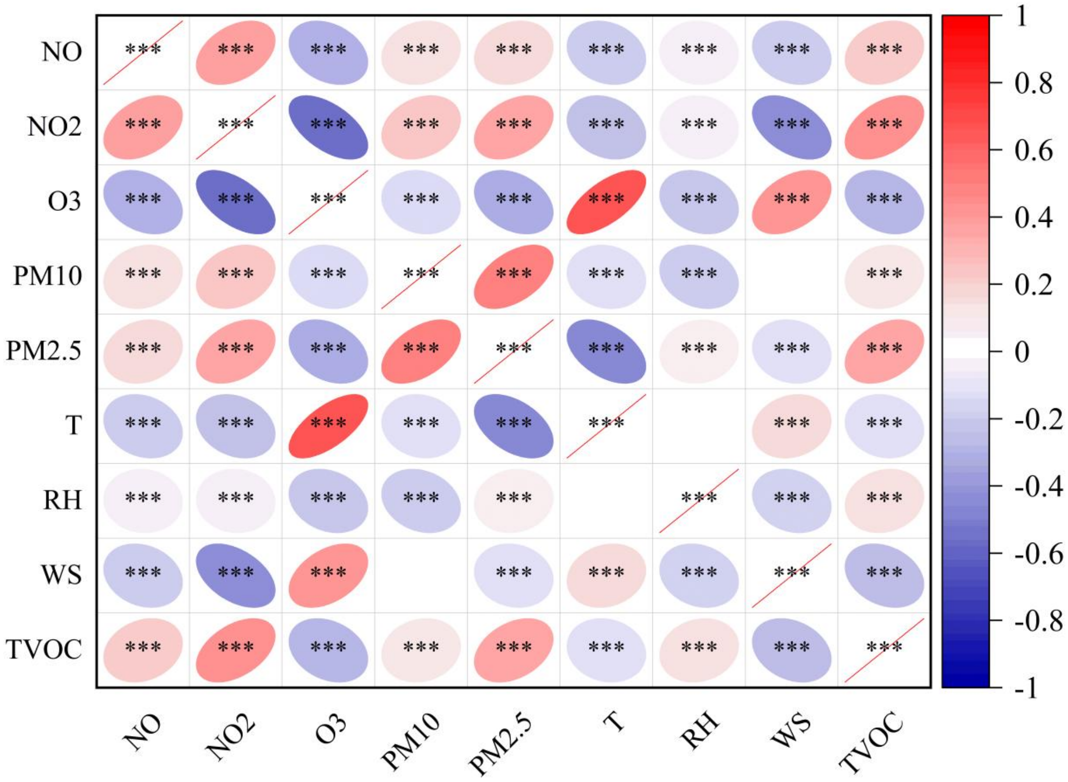

* p<=0.05 ** p<=0.01 *** p<=0.001

Fig.S3 Pearson correlation coefficients between pollutants and meteorological factors during the observation period.

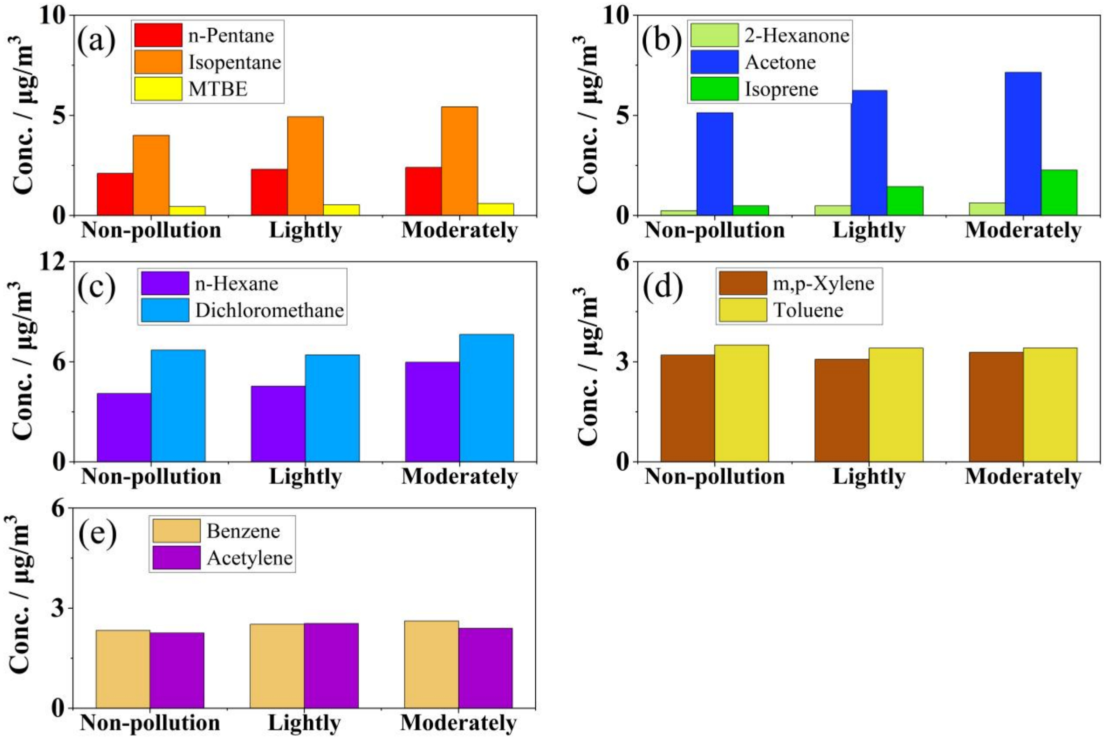

Fig. S4 Distribution of typical tracers for different pollutants.

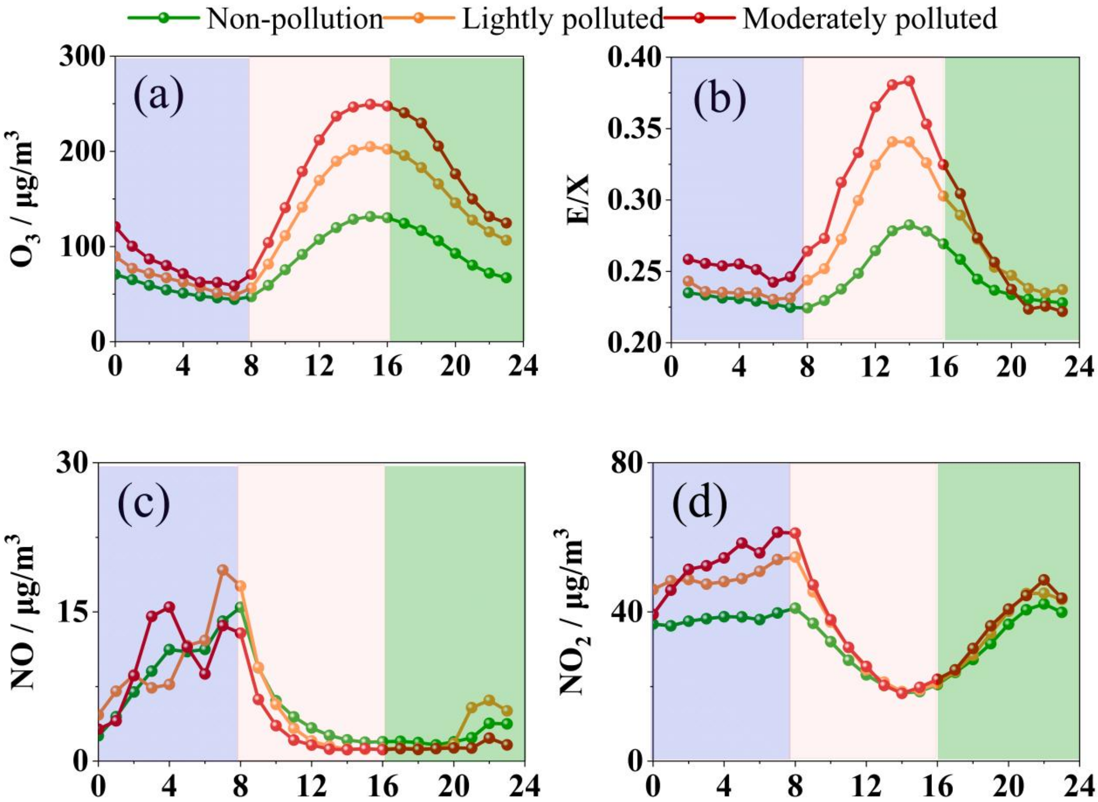

Fig. S5 Diurnal variation distribution of pollutants during different pollution periods. The light blue, light red, and light green shadows represent stages P1, P2, and P3, respectively.

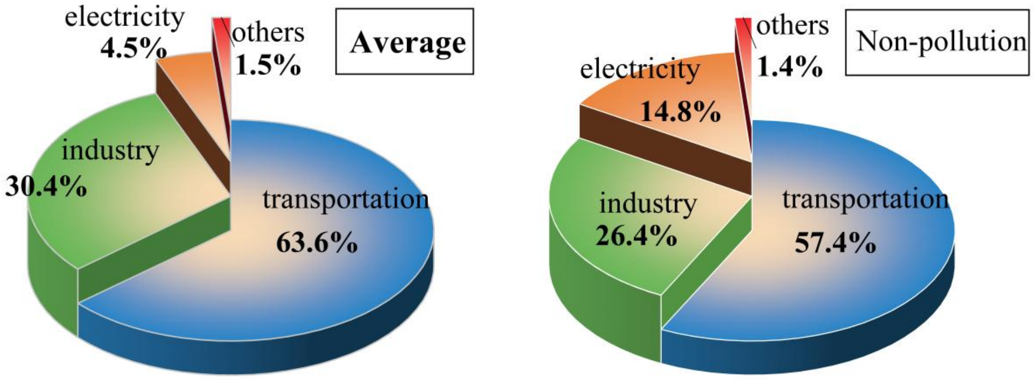

Fig. S6 The contribution of different sources to O_3 formation.

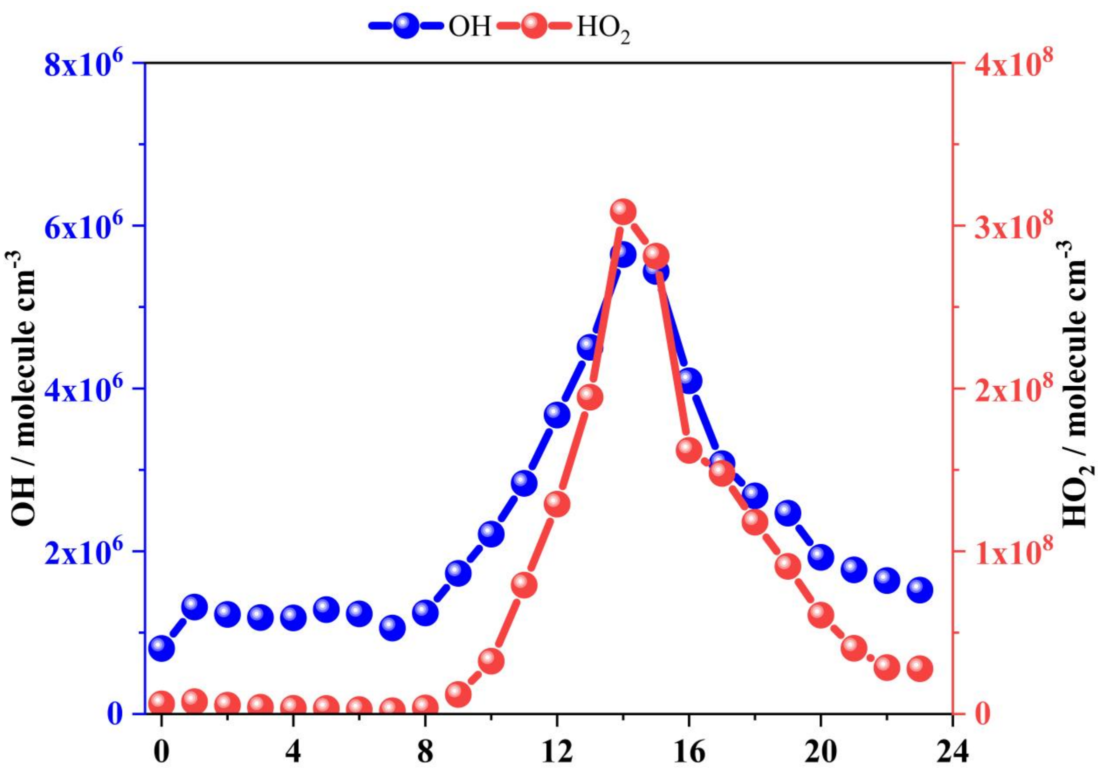

Fig. S7 Diurnal variation distribution of HOx radicals during the observation period.

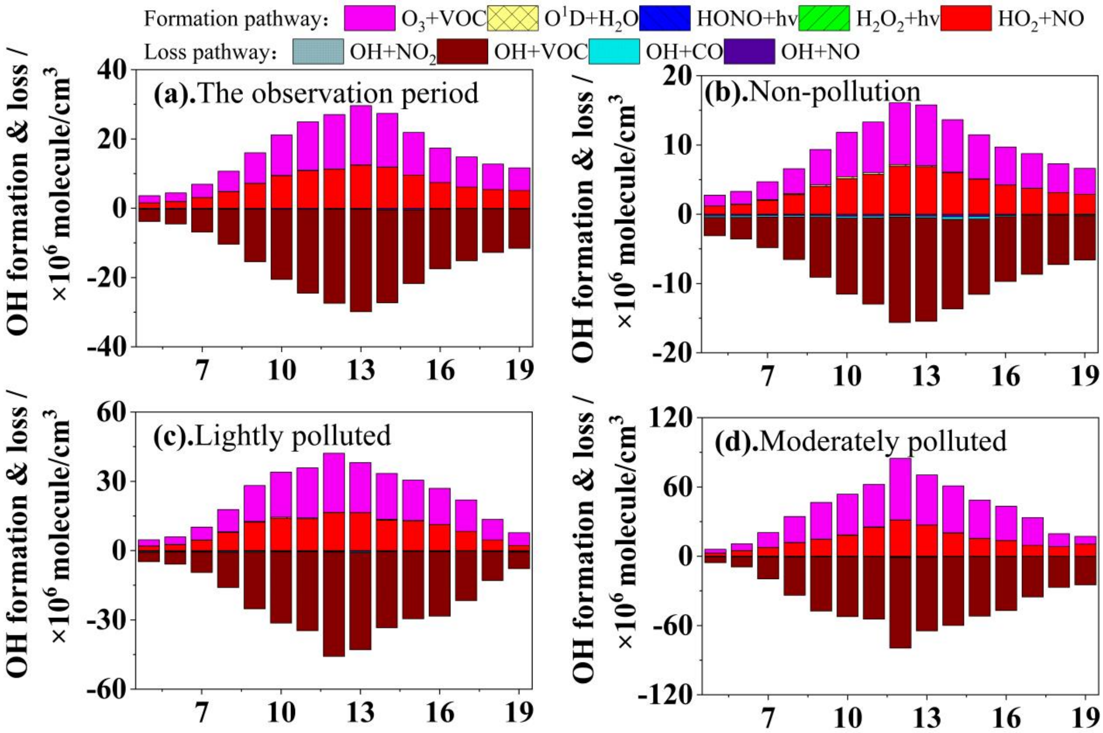

Fig. S8 Simulated average formation and loss rates of OH radicals at different pollution levels.

Table S1 Key parameter settings for the mode section.

Main parameters	Content
WRF Vertical resolution (eta_levels)	1.000, 0.996, 0.99, 0.98, 0.97, 0.96, 0.95, 0.94, 0.93, 0.92, 0.91, 0.895, 0.88, 0.865, 0.85, 0.825, 0.8, 0.775, 0.75, 0.72, 0.69, 0.66, 0.63, 0.6, 0.57, 0.54, 0.51, 0.475, 0.44, 0.405, 0.37, 0.33, 0.29, 0.25, 0.21, 0.175, 0.145, 0.115, 0.09, 0.065, 0.045, 0.025, 0.01, 0.000
Microphysics scheme	New Thompson et al. (scheme 8)
Longwave radiation	Rapid Radiative Transfer Model
Shortwave radiation	Goddard shortwave scheme
Land-surface scheme	Unified Noah land-surface model
Surface layer scheme	MYJ surface scheme
Boundary layer parameterization	Yonsei University scheme (Non-local -K scheme 1)

Table S2 Parameter table for O_3 simulation calibration in Henan Province

	$PM_{2.5}$	O_3
Normalized Mean Bias	0.30	-0.21
Normalized Mean Error	0.48	0.25
Mean Fractional Bias	0.21	-0.26
Mean Fractional Error	0.38	0.30
Correlation Coefficient	0.43	0.74

Table S3 Evaluating the robustness of the solution using bootstrap and displacement tests.

Diagnostics	3 factors	4 factors	5 factors	6 factors	7 factors
DISP % dQ	0	0	0	0	0
DISP % swaps	0	0	0	0	0
BS Mapping <80%			Factor 5 (62%)		Factor 5 (69%)
BS-DISP	Successful	Successful	Successful	Successful	Successful

Table S4 Performance metrics comparison between XGBoost and RF Models.

Model	Metric	Training Set	Test Set
XGBoost	R2	0.93	0.86
	MSE	0.07	0.13
	MAE	0.20	0.27
RF	R2	0.91	0.84
	MSE	0.08	0.15
	MAE	0.22	0.3

Table S5 Correlation analysis between pollutants and meteorological factors based on Kendall's method.

	O_3	NO	NO_2	PM_{10}	$PM_{2.5}$	T	RH	WS	VOCs
O_3	1								
NO	-0.415**	1							
NO_2	-0.460**	0.408**	1						
PM_{10}	-0.146**	0.243**	0.328**	1					
$PM_{2.5}$	-0.253**	0.251**	0.325**	0.514**	1				
T	0.483**	-0.294**	-0.183**	-0.110**	-0.313**	1			
RH	-0.147**	-0.110**	-0.036**	-0.199**	0.050**	-0.012	1		
WS	0.359**	-0.206**	-0.338**	-0.068**	-0.114**	0.125**	-0.123**	1	
VOCs	-0.305**	0.252**	0.435**	0.197**	0.306**	-0.084**	0.141**	-0.276**	1

Table S6 Correlation analysis between pollutants and meteorological factors based on Spearman's method.

	1	2	3	4	5	6	7	8	9	10	11	12
O_3(1)	1											
NO(2)	-0.648**	1										
NO_2(3)	-0.475**	0.624**	1									
PM_{10}(4)	-0.079**	0.278**	0.356**	1								
$PM_{2.5}$(5)	-0.262**	0.355**	0.544**	0.683**	1							
T(6)	0.839**	-0.579**	-0.401**	-0.168**	-0.394**	1						
RH(7)	-0.077**	-0.181**	-0.060**	-0.299**	0.061**	-0.021	1					
WS(8)	0.225**	-0.192**	-0.274**	0.039*	-0.102**	0.143**	-0.094**	1				
Alkanes(9)	-0.223**	0.317**	0.554**	0.297**	0.497**	-0.146**	0.090**	-0.218**	1			
Olefin(10)	-0.054**	0.122**	0.361**	0.147**	0.309**	0.143**	0.129**	-0.130**	0.612**	1		
Aromatic hydrocarbons(11)	-0.324**	0.393**	0.610**	0.131**	0.361**	-0.236**	0.115**	-0.192**	0.608**	0.477**	1	
Halogenated hydrocarbons(12)	-0.118**	0.182**	0.406**	0.060**	0.293**	-0.088**	0.243**	-0.117**	0.471**	0.436**	0.783**	1
OVOC(13)	0.221**	-0.133**	0.103**	0.055**	0.229**	0.254**	0.328**	-0.060**	0.541**	0.558**	0.449**	0.550**

Table S7 Comparative analysis of VOCs pollution characteristics in Zhengzhou and other cities.

No.	Time Period	Location	Site Type	VOCs Concentration	Dominant VOCs Species / Composition	Reference
1	May-Sep 2019-2021	Zhengzhou City, China	Urban site	90.3 ± 52.8 μg/m³	Dichloromethane, Acetone, Ethane, Isopentane, n-Hexane	This study
2	Summer 2019	Coastal Tokyo Bay, Japan (Yokohama area)	Industrial site (Ushioda)	86 μg/m³ (Range: 29–199 μg/m³)	Propane (6.9 μg/m³) > Ethyl acetate (6.0 μg/m³) > n-Butane (5.2 μg/m³) > Ethane (5.0 μg/m³) > Ethyl acetate (4.8 μg/m³)	Fukusaki et al., 2021
		Port-industrial mixed area (Yokohama Tower)	Port-industrial mixed site	70 μg/m³ (Range: 20–255 μg/m³)	Toluene (5.1 μg/m³) > Propane (4.9 μg/m³) > Ethyl acetate (4.8 μg/m³) > Ethyl acetate (3.8 μg/m³) > Ethane (3.5 μg/m³)	
3	Jan-Nov 2010	Greater Paris Metropolitan Area, France	Urban site	/	Alkanes: 39.1%, Oxygenated VOCs: 36.5%, Aromatics: 16.9%, Alkenes + Alkynes + Dienes: 7.5%	Baudic et al., 2016
4	[Data missing]	Beşiktaş District, Istanbul, Turkey	Urban site	40–60 μg/m³ (Average range)	Oxygenated VOCs: 43.9% (≈17 μg/m³), Alkanes: 26.3% (≈16 μg/m³), Aromatics: 20.7% (≈18 μg/m³), Alkenes: 4.8% (≈3 μg/m³)	Thera et al., 2019
5	Mar 2016 – Feb 2017	Athens, Greece	Urban site	50.3 μg/m³	Toluene: 6.7 μg/m³, Isopentane: 6.5 μg/m³, Ethane: 4.2 μg/m³, m/p-Xylene: 4.0 μg/m³, n-Butane: 3.8 μg/m³	Panopoulou et al., 2021
6	Jul 2022 – Apr 2023; Dec 2023 – Mar 2024	Vitória, Brazil	Urban site	24.1 ± 29.6 μg/m³	n-Pentane (4.59 μg/m³), Benzene (3.09 μg/m³), 1,2,4-Trimethylbenzene (1.49 μg/m³), Ethylbenzene (2.41 μg/m³)	Galvão et al., 2025
7	2017	Taiwan	Urban & industrial sites	53.4–76.0 μg/m³	Alkanes (46.5–55.3%) > Aromatics (28.0–42.2%) > Alkenes (7.4–11.4%) > Alkynes (1.2–5.5%)	Huang et al., 2020
8	Jan-Jul 2016	Beijing, Jing-Jin-Ji Region, China	Urban site	101.5 ± 65.2 μg/m³	Alkanes > OVOCs > Halogenated hydrocarbons > Aromatics > Alkenes > Alkynes	Liu et al., 2021
9	Jul-Dec 2019	Hefei, Yangtze River Delta Region, China	Urban site	68.79 μg/m³	Alkanes > OVOCs > Halogenated hydrocarbons > Aromatics > Alkenes > Alkynes	Wang et al., 2022

Table S8 Source analysis of VOCs in Zhengzhou and comparison with other cities.

No.	City/Location	Study Period	Site Type	PMF Source Apportionment (%)	Reference
1	Central Plains (Zhengzhou, Henan), China	Jan 2019-Sep 2021	Urban	Vehicle emissions: 32.4%; Solvent use: 24.8%; Industrial processes: 18.3%; LPG/NG combustion: 12.6%; Combustion sources: 8.9%; Biogenic: 3.0%	This study
2	Jing-Jin-Ji Region (Beijing), China	1 Jun-31 Aug 2020	Urban	Gasoline exhaust: 23.5%; Biogenic: 19.2%; Fuel evaporation: 15.7%; Diesel exhaust: 15.2%; Solvents: 14.3%; Industrial processes: 12.1%	Li et al., 2024
3	North China (Changzhi, Shanxi), China	2-30 Jun 2021	Urban	Gasoline vehicles: 27.0%; Coal combustion: 20.3%; Diesel vehicles: 15.9%; Industrial processes: 15.1%; Solvents: 14.0%; Biogenic: 7.6%	Niu et al., 2024
4	Yangtze River Delta (Suzhou, Jiangsu), China	2015-2022	Urban	Fossil fuel combustion: 20.4%; Solvents: 17.7%; Gasoline evaporation: 16.7%; Diesel exhaust: 12.6%; Natural gas: 10.8%; Industrial: 9.7%; Vehicle exhaust: 7.7%; Biogenic: 4.5%	Zhang et al., 2025
5	Yangtze River Delta (Tongxiang, Zhejiang), China	1 May-25 Jul 2021	Urban	Solvents & gasoline: 32.3%; Temperature-dependent sources: 28.1%; Vehicle exhaust: 19.9%; Manufacturing: 14.4%; Petrochemical: 7.8%	Qu et al., 2025
6	Taiwan Region (Taipei), China	Mar 2020-Feb 2021	Urban	Industrial solvents: 11.97-37.62%; Household emissions: 14.67-31.62%; Biogenic: 1.7-25.21%; Diesel vehicles: 5.74-19.03%; Petrochemicals: 5.43-18.67%; Gasoline vehicles: 4.51-12.34%	Chen et al., 2023
7	Vitória, Brazil (ES Site)	Jul 2022-Apr 2023; Dec 2023-Mar 2024	Urban site	Vehicle exhaust: 46%; Coke ovens: 26%; Solvents: 13%; Industrial processes: 11%; Fuel evaporation: 4%	Galvão et al., 2025
8	Paris Metropolitan Area, France	15 Jan-22 Nov 2010	Urban	Natural gas + background: 23%; Solvents: 20%; Wood burning: 17%; Vehicle exhaust: 15%; Biogenic: 15%; Gasoline evaporation: 10%	Baudic et al., 2016
9	Athens, Greece	3-26 Jul 2012 (Summer)	Urban	Traffic: 37.1%; Biogenic VOCs: 26.2%; Secondary oxidized VOCs: 19.3%; Biogenic oxidized VOCs: 18.4%	Kaltsonoudis et al., 2016
10	Beşiktaş District, Istanbul, Turkey	14-30 Sep 2014	Urban	Mixed area emissions: 36.3%; Natural gas evaporation: 25.9%; Road transport: 15.8%; Solvents (toluene): 14.2%; Biogenic terpenes: 7.8%	Thera et al., 2019

Table S9 Sensitivity distribution of O_3 pollution at different levels.

	VOCs/NOx	VOCs/NOx>10
Non-pollution	5.9 ± 7.3	8%
Lightly	7.0 ± 6.6	15%
Moderately	7.3 ± 6.7	18%